JOURNAL OF APPLIED ELECTROCHEMISTRY **27** (1997) 385–395

Applied studies on immobilized titanium dioxide films as catalysts for the photoelectrochemical detoxification of water

I. M. BUTTERFIELD, P. A. CHRISTENSEN*, A. HAMNETT, K. E. SHAW, G. M. WALKER, S. A. WALKER

The Chemistry Department, Bedson Building, The University, Newcastle upon Tyne, NE1 7RU, Great Britan

C. R. HOWARTH

The Department of Chemical and Process Engineering, Merz Court, The University, Newcastle upon Tyne, NE1 7RU, Great Britan

Received 20 January 1996; revised 3 June 1996

Preliminary results are presented on the photochemical and photo*electro*chemical degradation of aqueous organic solutions by anodic, thermal and sol–gel TiO_2 films. The films were tested in a photochemical falling film reactor, and a photochemical/photo*electro*chemical vortex reactor, and preliminary results are presented on the degradation of a range of model organics using these reactors. The former showed the best mass transport characteristics and most efficient light usage, whilst the latter reactor clearly showed the efficacy of the electric field enhancement effect. The results on the vortex reactor effectively represent a proof-of-concept of the electric field enhancement approach in large scale photoelectrochemical reactors. From time to time it is necessary to recoat the substrates, and the importance of the procedure adopted to remove 'old' TiO_2 films prior to the fabrication of 'new' films is highlighted, as well as the mode of operation of the sol–gel films, and problems encountered in reactor design.

1. Introduction

The potentially detrimental effects of trace chemicals in the environment have been well rehearsed in the literature, and a number of priority pollutants identified [1, 2]. However, it has become apparent that traditional methods of treating such polluted water, including adsorption [3] and oxidation [3–6], are becoming increasingly problematic.

The possible application of the powerfully-oxidizing $^{\bullet}OH$ radical in water treatment has led to the development of a suite of advanced oxidation processes, AOP [7], which for the most part generate $^{\bullet}OH$ radicals that can effect the complete mineralization of hydrocarbons to CO_2 and H_2O, and halocarbons to these and mineral acids.

It is known that the irradiation of TiO_2 with supraband-gap light (3.2 eV) leads to the generation of $^{\bullet}OH$ radicals at its surface, and the potential of TiO_2 to effect the detoxification of water was first exploited in slurry reactors [7–10].

On irradiation of a TiO_2 particle with supraband gap light, a photogenerated electron-hole pair is formed, and there is a finite possibility that the electron and hole will overcome their mutual electrostatic attraction and become spatially separated. These will then diffuse to the surface where the electron will be captured by O_2, and the hole by adsorbed hydroxide to form $^{\bullet}OH$ radicals. However, before the electrons and holes reach the surface, there is a significant chance of recombination, and this is an important source of inefficiency in systems employing semiconductor catalysts for photochemical conversion of light [11]. The minority carrier length, L_p, in TiO_2, that is, the distance the holes move in a field-free region before recombination with an electron, is about 0.1 μm [12].

The use of the TiO_2 catalyst in the form of a slurry does have the great advantage of having good mass-transport characteristics. However, L_p must be comparable to, or greater than, the particle size if charge recombination is not to be a limiting factor, and hence there is a severe restriction on the size of the semiconductor particles. Unfortunately, if the slurry employs such very fine particles, then this, in turn, requires very long settlement times for the catalyst to be removed from the purified water; alternatively, fine filters must be employed. In either case, a severe restriction is placed on the throughput of the treatment process. Consequently, attention has recently turned to the application of immobilized catalysts [13–15], usually in the form of TiO_2 powder attached to the sides of a vessel, which constitutes a flow-through reactor. The use of the photocatalyst as an immobilized film clearly has attendant mass transport problems compared to the suspension. In addition,

* Author to whom correspondence should be sent.

0021-891X

there is a problem with the efficiency of light absorption by a thin film since TiO_2 has a low absorption coefficient at energies near that of the band gap. In the case of a slurry of TiO_2 particles, this is not a problem as it is possible to ensure that all the incident light is absorbed simply by having a large number of particles present. This is not the case for a TiO_2 film. If the film is too thick, the most of the holes are generated too deep in the bulk of the semiconductor and never reach the surface; conversely, if the film is too thin, then very little of the incident light will be absorbed.

The light absorption problem can be offset to a certain extent by either (i) employing a porous TiO_2 film and so ensuring maximum light absorption, but with the holes never being generated too far from the surface; or by (ii) imposing a potential bias on the semiconductor film, and exploiting the electric field enhancement (EFE) effect. Providing that the electrolyte concentration is larger than the film dopant density, the application of a positive potential bias to a TiO_2 film generates an electric field to a depth W, termed the depletion layer, within the semiconductor, see Fig. 1. This internal electric field is highly dependent upon the degree of doping, and can arise from the presence of immobilized negative charge on the semiconductor surface, as well as from the application of a positive bias. The presence of this electric field greatly facilitates the process of charge separation [16], and this photo*electro*chemical effect, the EFE effect, is depicted in Fig. 1.

The maximum penetration depth of the incident light into TiO_2 is $1/\alpha$, where α is the absorption coefficient of the TiO_2 at the wavelength of the incident light. Any holes generated in the depletion layer W will be efficiently transported to the surface. Holes generated still deeper, at a depth of between W and $(W + L_p)$, may diffuse to the depletion layer boundary, and will then also undergo efficient transport to the surface. Absorption of radiation at depths $>(W + L_p)$ will result in charge recombination. The conduction band electrons are drawn away from the semiconductor film, and can migrate to a suitable counter electrode, allowing the counter electrode reaction, (usually oxygen reduction), to be driven separately, so preventing the build up of negative charge at the semiconductor surface. For reasonable dopant levels within the TiO_2 layer, ($\geq \sim 10^{17}$ cm^{-3}), and in reasonably conducting electrolytes, the magnitude of the internal electric field, even at a bias of $\sim$ 1V, is sufficient to separate photogenerated electrons and holes efficiently.

From the above discussion, it can be seen that the application of a potential bias to a TiO_2 film should lead to an improvement in the efficiency of the photooxidation process. As an example, Vinodgopal *et al.*[17, 18] and Kim and Anderson [19] have reported that the photochemical degradation of 4-chlorophenol and formic acid, respectively, by immobilized TiO_2 films was enhanced by the application of an electric field across the semiconductor.

One consequence of the potentially high surface concentration of $^{\bullet}OH$ radicals at the TiO_2 surface is that the evolution of oxygen can be a significant parasitic reaction. The rate of this reaction has been postulated [20–23] as being a function of the concentration of oxygen vacancies. The oxygen evolution reaction is clearly an undesirable side reaction, and hence it is important that films are fabricated that minimize the number of oxygen vacancies. To this end, the methods of producing the n-TiO_2 films were first assessed using small (0.4 cm^2) Ti electrodes as substrates. These films were characterized using cyclic voltammetry, (to measure photocurrent), and *in situ* FTIR, (to measure activity and selectivity towards organic oxidation, as well as the efficiency of the mineralization process) [24]. After this initial study the fabrication techniques that were found to generate reasonably active and selective films were employed on a significantly larger scale for testing in the photoreactors.

The aim of work reported in this paper was to design, build and assess large-scale reactors for the photoelectrochemical detoxification of water using immobilized TiO_2 catalytic films. Implicit within this aim are three objectives: (i) to establish techniques to fabricate large, active films of TiO_2, (ii) to overcome the significant mass transport problems associated with the application of an immobilized catalytic film, and (iii) to assess whether the electric field enhancement effect is observed in such large scale reactors and, if so, to what extent it can be exploited to improve the efficiency of the detoxification process.

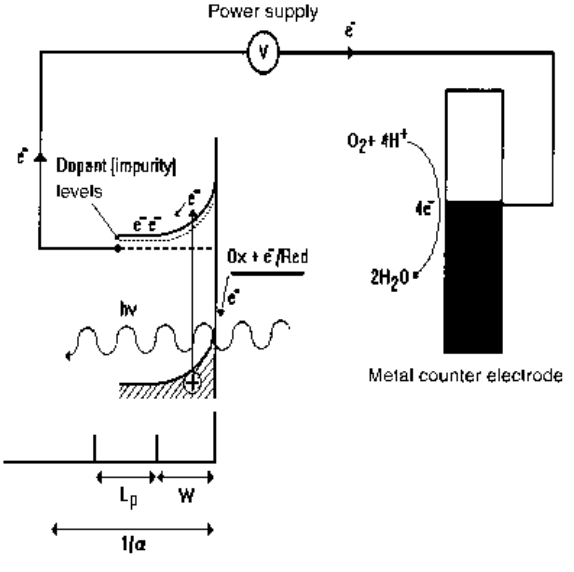

Fig. 1. Schematic representation of the events taking place during the irradiation of a n-doped semiconductor immersed in aqueous solution and under a positive potential bias, with suprabandgap light. The penetration depth of the light is $1/\alpha$, where α is the absorption coefficient of the semiconductor at the wavelength of the light; W is the depletion layer width, and L_p is the distance the minority carriers (i.e., holes in n-TiO_2) move in a fieldfree region before recombination.

2. Experimental details

2.1. *Chemicals*

Titanium isopropoxide (97%, Aldrich), ethanol (anhydrous and denatured, Aldrich), sodium formate (Aldrich), phenol and 4-chlorophenol (BDH AnalaR), $NaClO_4$ (Mercke AnalaR) and salicylic acid (BDH) were used without further purification. Acids employed were of analytical grade. Water used in the reactions was deionized using a Milli-Q water purification system (Millipore Corp, 18 MΩ cm).

The model organics were selected because of their presence on list of priority pollutants and/or because of their being representative of materials routinely studied in the literature.

2.2. *Preparation of the TiO_2 sol–gel films*

The TiO_2 sols were prepared in an acid-catalysed reaction by mixing titanium isopropoxide with half the prescribed volume of ethanol. The remaining ethanol was mixed with water which had been acidified with hydrochloric or nitric acid, this latter ethanolic solution was then added slowly to the former solution under constant stirring. The chemical composition of the starting alkoxide solution was $Ti(O\text{-}i\text{-}C_3H_7)_4$:$H_2O$: C_2H_5OH: HCl = 1: 1: 8: 0.008 in molar ratio [25] and it was left standing for a period of at least one hour allowing the room temperature hydrolysis reaction to take place and ensuring TiO_2 sol formation.

TiO_2 films were applied to substrates using the dip-coating technique which involves immersing the substrate into the sol and slowly withdrawing it. This procedure resulted in an adsorbed amorphous TiO_2 film on the substrate, which was then converted to a microcrystalline anatase film by heating at 500 °C for 10 minutes in air. Loose TiO_2 particles were then removed by vigorous rubbing with a paper towel. The desired film thickness was obtained by repeating the above method, usually to a total of 10 'dips'.

2.3. *Preparation of anodic TiO_2 films*

The anodic films were fabricated by the slow growth method, as described by Smyrl [26]. The titanium plate, after cleaning with ethanol to remove adventitious grease etc., was employed as the working electrode in a three-electrode cell, with a stainless steel plate as the counter electrode, and using an SCE as reference. The electrolyte employed was 1 M NaOH, and the film was grown by increasing the potential at 0.1 mV s^{-1} from −0.83 V (the open circuit potential) to 9 V. Taking the anodizing ratio to be 3 nm/V [27], the film thickness was estimated to be 29.5 nm.

2.4. *Preparation of the thermal films*

The titanium plate was cleaned with ethanol before being placed in a furnace preheated to 630 °C for 20 min in air, after which it was allowed to cool slowly. Thermal films formed by such a method have been found to be active towards the photoelectrochemical splitting of water [28].

2.5. *Ultraviolet*

A 400 W medium pressure Hg lamp (Photochemical Reactors Ltd), and a 2.5 kW Hanovia Hg lamp were employed.

2.6. *Experiments using the falling film and vortex reactors*

The destruction of the model contaminants; 4-chlorophenol, phenol, salicylic acid and sodium formate were observed in all the reactors. The degradation of the model contaminants and the generation of their intermediates were followed by HPLC (Philips Pye Unicam PU4010 pump and PU4020 u.v. detector, sample volume of 20 μL) using Waters Novapack C_{18} columns. The mobile phase employed was 75% H_2O, 24.5% CH_3CN and 0.5% H_3PO_4 (by volume). This was pumped through the column at a rate of 15 cm^3 min^{-1}, and detection was by means of a u.v. detector at 280 nm. The sampling time scales varied for both reactors.

The main requirements for a reactor to be used in photoelectrocatalysis with conducting immobilized catalysts are: turbulent flow to allow good mass transport of organic species to the catalyst surface, a residence time long enough to enable good conversion rates of organics whilst still achieving a high enough throughput and the ability to apply a potential bias across the system.

2.6.1. Falling film reactor. As a result of the difficulties encountered in trying to apply a biasing potential to the TiO_2 film in the falling film reactor (FFR), it was only employed in purely *photo*chemical studies. The FFR consisted of a stainless steel pipe (80 cm length and 10 cm diameter) coated on the inside surface with a TiO_2 sol–gel film. The film was illuminated by a u.v. light tube (2.5 kW, Hg) inserted down the axis of the pipe. The pipe and u.v. source were held vertically and a continuous thin, well mixed film of aqueous organic contaminant was sprayed into the top of the pipe and collected at the base where it was bubbled with air (ensuring continuous organic mixing) prior to being pumped back to the top of the pipe, see Fig. 2. The reactor has an operating volume of 10 dm^3 and was operated at a flow rate of 5 dm^3 min^{-1}. Samples for HPLC analysis were taken at regular intervals.

2.6.2. Vortex reactor. The vortex design is more commonly employed a fluidic in-line mixer [29], and one of the major advantages of this design is that it has no moving parts, and was readily adapted into a photo*electro*chemical system. Two vortex reactors were employed. The first having a 30 cm diameter

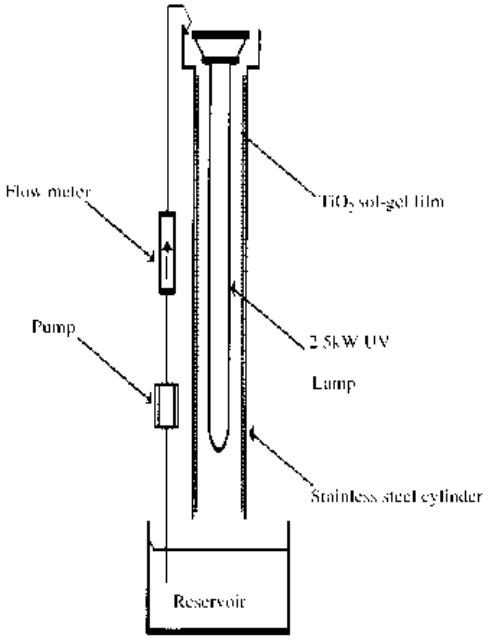

Fig. 2. Schematic diagram of the falling film reactor (FFR).

electrode, and the second, designed in conjunction with British Nuclear Fuels Ltd (BNFL), having a 45 cm diameter working electrode.

As can be seen from Fig. 3, the liquid effluent enters the vortex reactor through tangential ports, (two for the smaller 30 cm diameter design, up to four for the larger 45 cm design), situated above the TiO_2 - coated working electrode. A counter electrode, made of nickel mesh or wire, was then placed parallel to the working electrode at a distance of 1 cm, and allowed u.v. illumination from above. In the case of the nickel wire counter electrode 1 mm diameter wire was spot welded to form a grid with approximately 5 cm × 5 cm open squares, while the nickel mesh counter electrode was woven mesh of 0.5 mm diameter with

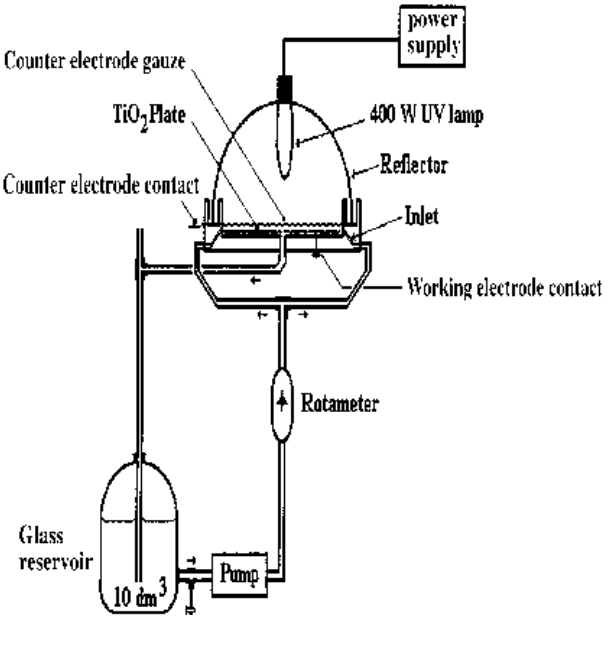

Fig. 3. Schematic diagram of the vortex reactor (VR).

approximately 50 % open area. The counter electrode is approximately 10 % of the area of the working electrode. The liquid moves around the reactor in vortex flow until it reaches the outlet in the centre of the reactor, when it is returned to the holding reservoir. The flow rate of the effluent determines the thickness of the solution above the working electrode, and is controlled by a rotameter. The reactor is essentially a multipass system.

The 30 cm diameter reactor was constructed from polypropylene in two halves, with the working electrode sitting in the bottom half of the reactor. The larger reactor was fabricated from a single piece of polypropylene. In the smaller reactor, the counter electrode was held cofacial with the working electrode plate by means of a polypropylene ring attached to the bottom half of the reactor by screws. In the larger reactor, the counter electrode consisted of nickel gauze sheets maintained at a distance from the working electrode by nylon 'feet'. The nickel mesh counter electrode was placed as close as possible above the photocatalyst to ensure even potential distribution across the working electrode surface, and thus minimize *iR* drop effects, permitting a homogeneous reaction profile across the working electrode surface. Where appropriate a bias potential was applied to the working electrode (TiO_2 - coated titanium plate, 30 cm in diameter) *via* a ministat (Sycopel) and precision potentiostat (Sycopel).

The flow rate employed using the smaller reactor was typically 10–14 $dm^3\ min^{-1}$, and that in the larger reactor typically 2–4 $dm^3\ min^{-1}$, giving a mean residence time of 6 s and 15 s, respectively.

The flow in the vortex reactors was observed by placing dye in the solution to check that a good vortex pattern was observed, and that the majority of the flow was not simply moving straight from inlet to outlet.

The output intensity of the 400 W lamp employed in both reactors was determined using ferrioxalate actinometry [30], and found to be 1.3×10^{15} photons $s^{-1}\ cm^{-2}$ reaching the solution.

3. Results

The project commenced with a falling film reactor, (FFR), as this reactor was of the simplest design, (and so relatively easy to fabricate). It showed the most efficient mass transport properties and light usage compared to the vortex reactors and, it was hoped, would therefore provide a useful initial benchmark with which to compare photochemical and photelectrochemical performance.

This section will be divided according to reactor type, rather than film type. To a certain extent, the reactor type was dictated by the films that could be studied, with both the falling film reactor and the 45 cm diameter vortex reactor being too large to allow the fabrication of anodic films. This was due to the fact that the currents required during the growth protocol required d.c. power supplies and control systems that were not available to us.

3.1. *Falling film reactor*

Figure 4 shows the degradation of phenol, 4-chlorophenol and salicyclic acid in the falling film reactor, using a sol–gel film and without any added electrolyte.

As can be seen, 4-chlorophenol is degraded rapidly, with phenol and salicylic acid rather less so. Figures 5(a) and (b) show results on the degradation of phenol obtained on the falling film reactor (a) in the absence of the sol–gel TiO_2 film, and (b) in the presence of the film.

Degradation of the phenol occurs in both the experiments, although rather more rapidly in the presence of the photocatalytic film. A rather more marked difference can be seen in terms of the intermediates produced in both experiments. In the blank (light only) experiment, Fig. 5(a), appreciable quantities of quinol and catechol are produced, ~20 μM of each, after 2 h irradiation. In the presence of the sol–gel film, however, the intermediates are apparently mineralized.

These results are quite promising; however, the very high power of the u.v. lamp is clearly a significant disadvantage in terms of the cost of the detoxification process. One possible approach to reducing the lamp power is to take advantage of the potential increase in efficiency afforded by the electric field enhancement effect, and convert the photochemical FFR into a photo*electro*chemical system by placing a counter electrode cofacial to the TiO_2-coated working electrode. Unfortunately, the very thin solution layer and curved geometry of the cylindrical reactor rendered such a modification impossible. Consequently, it was decided to modify an exiting electrochemical reactor, a vortex reactor, to allow irradiation of the working electrode. It was hoped that the electric field enhancement effect would then allow a lower power lamp to be employed, and a 400 W Hg lamp was chosen to carry out the preliminary work intended to determine if the electric field enhancement effect could be exploited.

3.2. *Vortex reactor*

(a) *30 cm diameter disc reactor*. Clear evidence for the electric field enhancement effect when using electrolyte-containing solutions was obtained using sodium formate and phenol in neutral 0.1 M $NaClO_4$, and employing a sol–gel TiO_2 film, see Figs 6 and 7.

In the absence of the TiO_2 film, little or no degradation of the formate was observed over 60 min, see Fig. 6(i). However, repeating the experiment in the presence of the catalytic film at open circuit resulted in a ~11% mineralization of formate. Using the film and a + 1.0 V vs SCE applied potential resulted in ~ 24% of the organic being mineralized.

The same trend was repeated in the phenol experiment, except that appreciable amounts of intermediates were formed. Figure 7 shows the results of similar experiments to those depicted in Fig. 6, and Table 1 lists the amounts of the quinol and catechol intermediates produced compared to the amount of phenol degraded at the end of 60 min irradiation in each case in Fig. 7.

In contrast to the case of formate, appreciable degradation of phenol takes place in the blank experiment using the u.v. lamp only; 16% of the phenol is degraded, of which a total of one third is converted only as far as catechol and quinol. On employing the TiO_2 sol–gel film at open circuit, the degradation rises to ~27%, of which roughly one half has been converted to intermediates. Finally, when the TiO_2 was

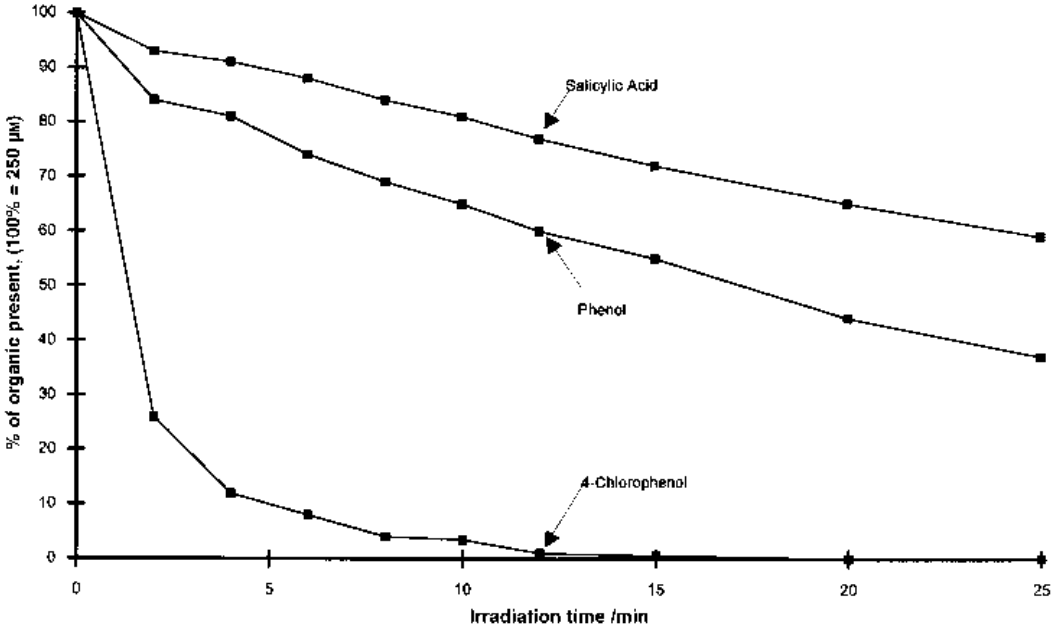

Fig. 4. Percentage of organic present as a function of irradiation time for the degradation of salicylic acid, phenol and 4-chlorophenol in the falling film reactor with a sol–gel TiO_2 film; 100% = 250 μM in 10 dm^3 of water. Catalyst area ~ 800 cm^2, flow rate 5 dm^3 min^{-1}, 2.5 kW mercury lamp.

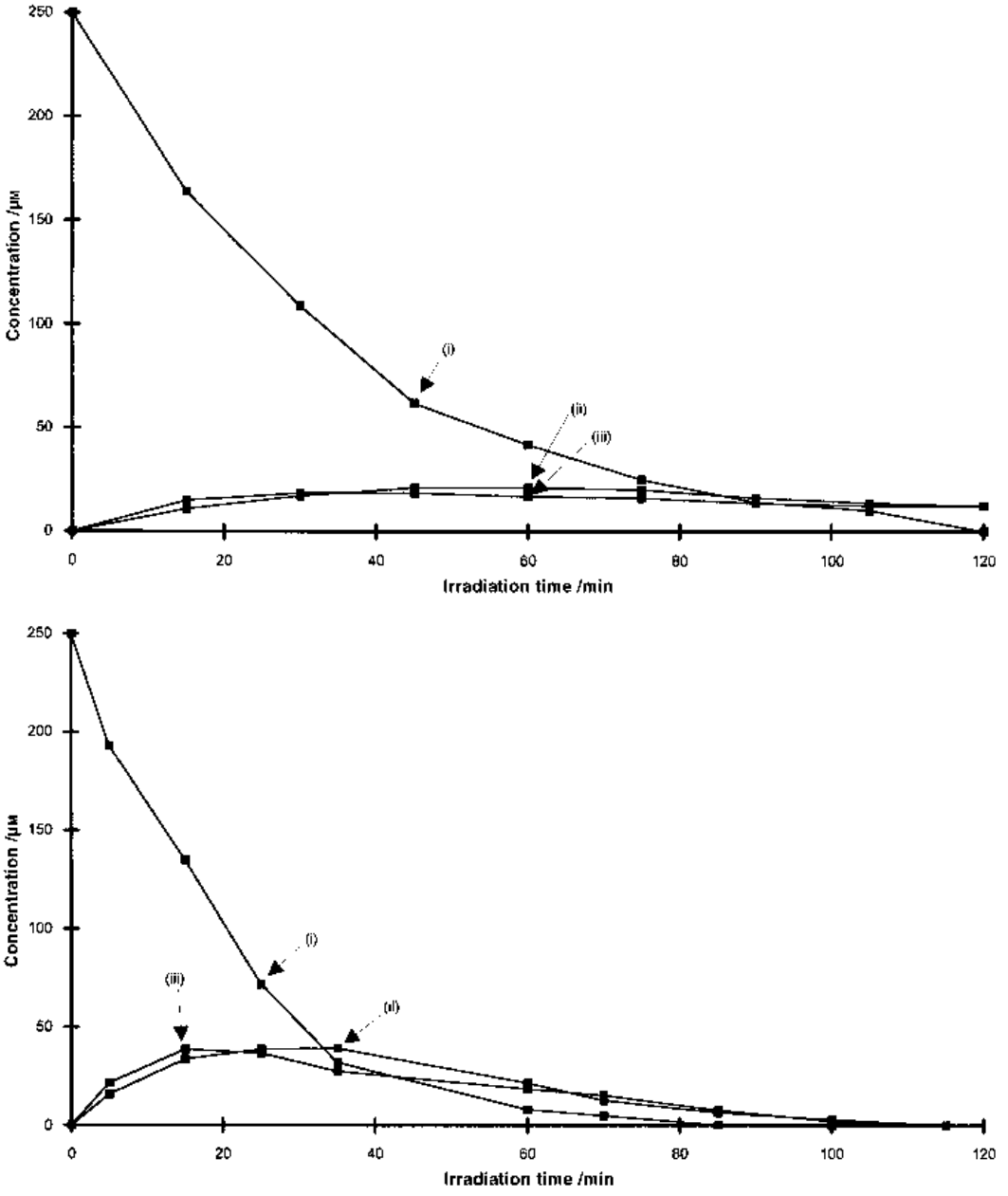

Fig. 5. (a) Concentration of (i) phenol, (ii) catechol and (iii) quinol present as a function of irradiation time in the falling film reactor in the absence of a photocatalytic film. (b) Repeat of the experiment in Fig. 5(a) in the presence of the photocatalytic sol–gel TiO_2 film in Fig. 4. Reservoir contained 250 μM phenol in 10 dm^3 of water. Catalyst area ~800 cm^2, flow rate 5 dm^3 min^{-1}, 2.5 kW mercury lamp.

employed with a + 1 V bias, 34% of the phenol was degraded, with one third again going to intermediates. In all of these experiments the photocurrent density was typically 500 μA cm^{-2}.

Interestingly, in the absence of any added electrolyte, the results observed were very similar to those in Fig. 7 and Table 1.

At first sight, it is surprising that a sol–gel TiO_2 film should exhibit such a marked EFE effect, since it would be expected that the film would be generated in a very lightly doped form. However, the films appeared very dark to the eye, suggesting appreciable carbon content, a hypothesis supported by *in situ* FTIR measurements [24]. Yoko *et al.* [31] attributed

Table 1. Percentage loss of phenol and percentage gain of intermediates for the experiment in Fig. 7 after 60 min irradiation

Experiment	*Loss of phenol* /%	[*Moles catechol gained*]/ [*Moles phenol lost*]/%	[*Moles Quinol gained*]/ [*Moles phenol lost*]/%
Blank, (u.v. only)	16	19	15
TiO_2, open circuit	27	25	21
TiO_2, +1V	34	19	12.4

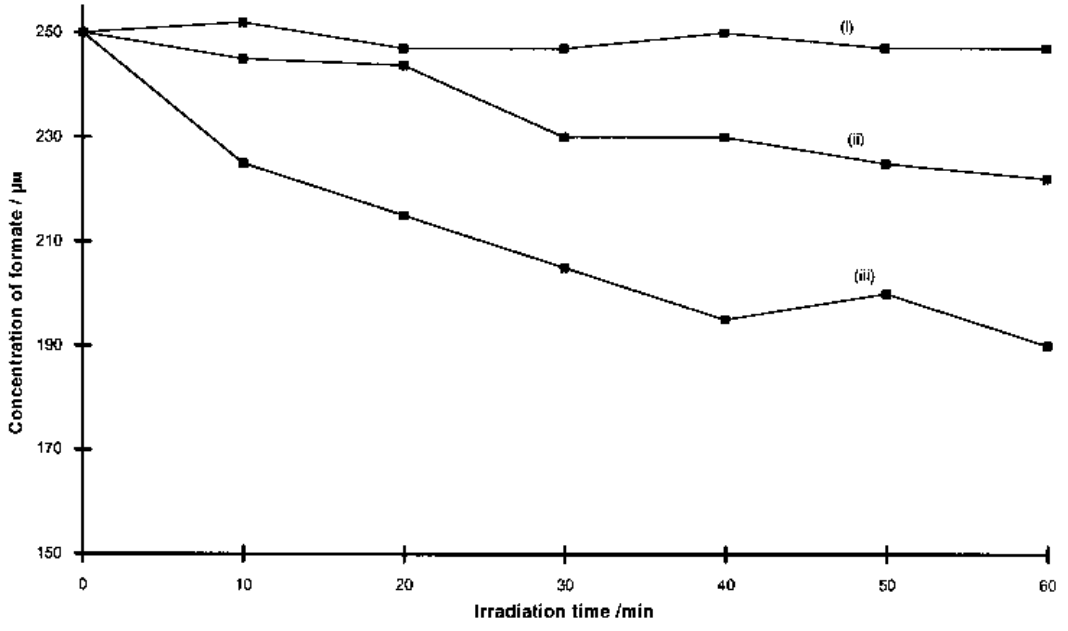

Fig. 6. Concentration of formate present as a function of irradiation time in the vortex reactor (i) in the absence of a photocatalytic film, (ii) in the presence of the sol–gel TiO_2 film at open circuit and (iii) at +1.0 V vs SCE. Reservoir contained 250 μM sodium formate in 10 dm^3 of aqueous 0.1 M $NaClO_4$. Catalyst area ~ 707 cm^2, flow rate 4.5 dm^3 min^{-1}, 400 W mercury lamp.

this dark colour to adventitious doping arising from the reducing action of undecomposed residual carbon remaining within the film. However, our results (see below) suggest that the sol–gel films are a heterogeneous mixture of TiO_2 and carbon, with electronic conductivity taking place through both components.

The anodic film in aqueous 0.1 M $NaClO_4$ gave similar results to those obtained with the sol–gel film described above. Again, there was clear evidence for the EFE effect, with ~36% of phenol being degraded over 60 min at open circuit, compared to 48% degradation at +0.5 V. At open circuit, ~32% of the degraded phenol was converted to catechol and resorcinol, and 20% to hydroquinone. At +0.5 V, 21% of the degraded phenol was converted only as far as catechol and resorcinol, and 7% to hydroquinone.

(b) *45 cm diameter disc reactor*. Thermal films were not investigated in the smaller VR due to time limitations. However, they were investigated in the scaled-up version of the VR. Figure 8(a) and (b) show results obtained with a 45 cm diameter thermal film and 778 μM 4-chlorophenol in 5 dm^3 of water.

There is very little increase in degradation over the blank (light only) on employing the TiO_2 film at open

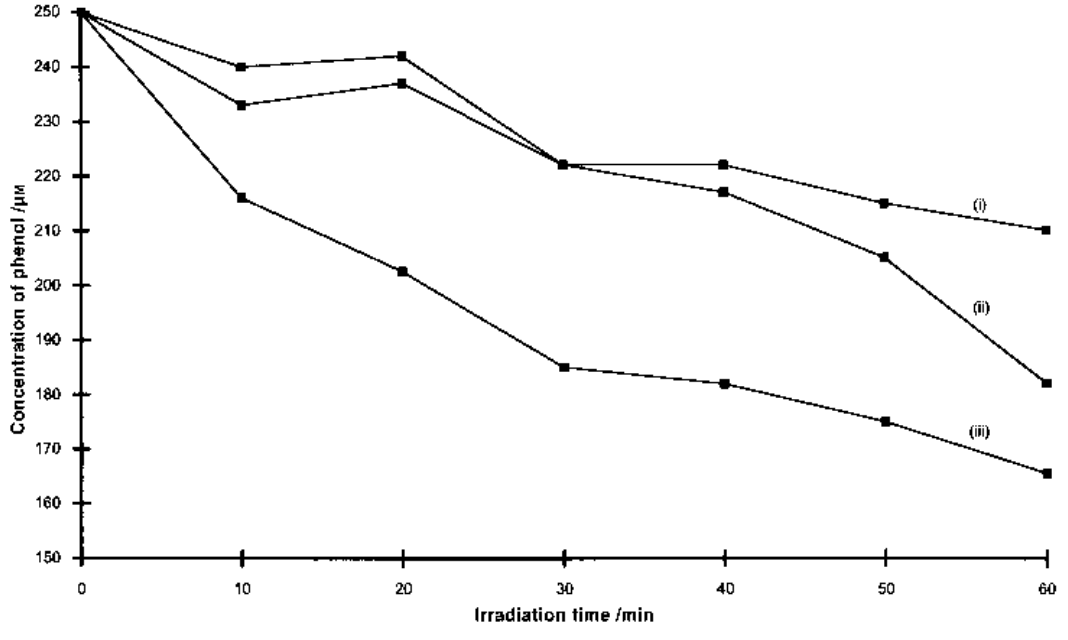

Fig. 7. Repeat of the experiment in Fig. 6, except using phenol.

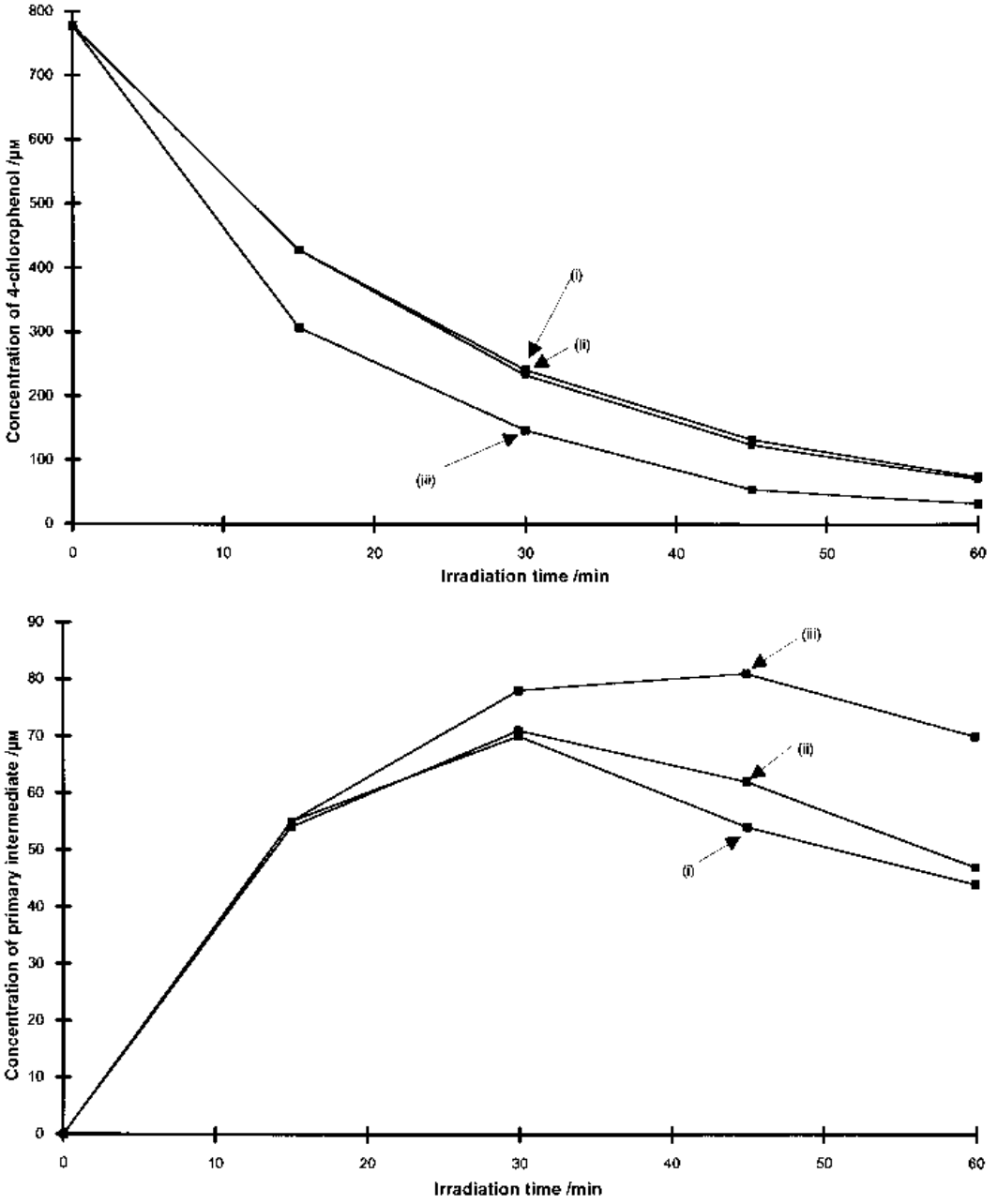

Fig. 8. (a) Concentration of 4-chlorophenol present as a function of irradiation time in the larger vortex reactor (i) in the absence of a photocatalytic film, (ii) in the presence of a thermal TiO_2 film at open circuit and (iii) at +1.0 V vs SCE. Reservoir contained 778 μM 4-chlorophenol in 5 dm^3 of water. Catalyst area ~ 1590 cm^2, flow rate 2.0 dm^3 min^{-1}, 400 W mercury lamp. (b) Concentration of phenol intermediate as a function of time for the experiments shown in Fig. 8(a). (i) In the absence of a photocatalytic film, (ii) in the presence of a thermal TiO_2 film at open circuit and (iii) at +1.0 V vs SCE.

circuit. However, there is a clear increase on applying a +1.0 V bias to the film. When the thermal film investigated in this experiment was removed, by mechanical polishing with an orbital sander, (as the plates were too large to be mounted in a lathe for a cutting tool to be employed), the films grown subsequently on the polished substrates were found to be inactive towards organic oxidation, even though the same growth protocol had been employed. The same result was observed for the anodic films.

The amounts of intermediate produced in the blank and open circuit runs in Fig.8(b), curves (i) and (ii), are approximately the same within experimental error; whilst the +1.0 V run shows an increase. Figure 8(a) shows the same kind of behaviour, with the rate of degradation of the blank experiment tracking that in the open circuit run, whilst the +1.0 V experiment shows a faster degradation rate. This suggests that the increasing amount of intermediate observed at +1.0 V is simply a result of the increased amount of degradation.

The sol–gel films gave similar results to those obtained in the smaller VR reactor. However, if they were fabricated on a substrate after it had been polished, they also gave somewhat different results. Figure 9 shows the degradation of 4-chlorophenol in the larger VR using a sol–gel film grown on a polished titanium substrate, (*cf.* Figs 6 and 7).

4. Discussion

It is clear that the results presented in this paper effectively represent a proof-of-concept of the EFE approach applied to large-scale photoelectrochemical reactors, with the application of a potential bias to an anodic, sol–gel or thermal TiO_2 film causing an increase in the degradation of the model organics compared to the open circuit and light-only experiments.

While it is also clear that it is possible to effect the mineralization of organics using the photochemical falling film reactor, this efficiency is probably due to the high power of the u.v. lamp employed, and the highly turbulent nature of the thin effluent film. In the case of the vortex reactors, degradation of the chosen organics is significantly slower, and complete mineralization is not assured with the current configuration over periods of ~1 h. A system requiring long irradiation times using a 400 W lamp is clearly not going to be commercially attractive.

Both vortex reactors employed an open configuration, that is, the liquid layer over the working electrode was not constrained to a maximum thickness. This had two detrimental effects: (i) the flow characteristics of the reactor could not be modelled, and (ii) the minimum solution thickness attainable in the smaller reactor was ~0.5 cm, and in the larger reactor was ~1.0 cm. Such large thicknesses are not conducive to efficient mass transport, and can cause problems with light absorption by the organic significantly reducing the light intensity incident on the catalyst surface.

The surface area of the counter electrode also poses a problem. Clearly, from an electrochemical point of view, this should be as high as possible and cofacial with the working electrode. Mavroides *et al.* [32] employed a counter electrode 50 × the area of their TiO_2 electrode in their experiments on the photoelectrochemical splitting of water, in order to ensure that the counter electrode reaction, hydrogen evolution or oxygen reduction, was not limiting. Taking these facts together, and with the requirement that the counter electrode should block the minimum amount of light from reaching the electrode, places severe restrictions upon the design of large scale photoelectrochemical reactors. These were not, in essence, overcome in the work reported in this paper; rather, a compromise was reached.

The experiments reported in this paper were all intended as preliminary work aimed at assessing all aspects of the reactors, including the electrochemical characteristics. Consequently, they all employed the three-electrode configuration, including a reference electrode. The position of the reference electrode luggin was not found to be too critical in the smaller vortex reactor, so long as it was passed through the counter electrode and held reasonably close to the TiO_2 film surface. However, this was not the case for the larger vortex reactor. If the reference electrode luggin was anywhere except over one of the contact points to the working electrode, the potential of the working electrode was found to vary widely. In these circumstances, damage to the film resulted, with areas being reduced apparently to the bare metal in patterns exactly matching the pattern of the counter electrode above, and the nickel counter electrode suffering concommittant oxidation.

The effect of polishing the titanium substrates prior to film formation is interesting. Subsequent enquiries of the suppliers revealed that the titanium sheets employed by us as substrates are manufactured

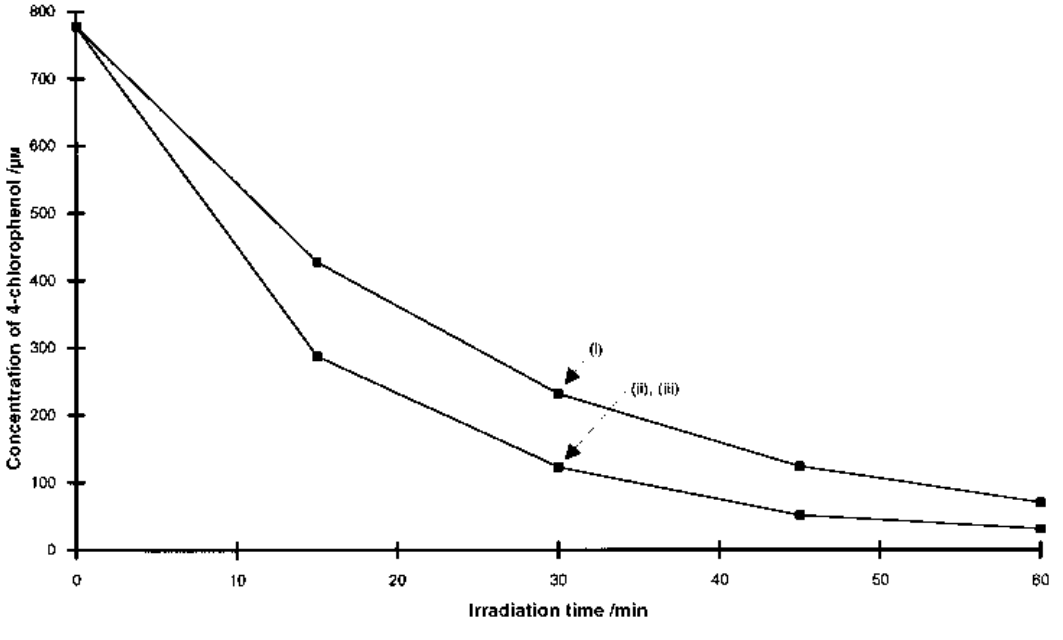

Fig. 9. Concentration of 4-chlorophenol present as a function of irradiation time in the larger vortex reactor (i) in the absence of a photocatalytic film, (ii) in the presence of a sol gel TiO_2 film on a *polished* Ti substrate at open circuit and (iii) at +1.0 V vs SCE. Reservoir contained 778 μM 4-chlorophenol in 5 dm^3 of water. Catalyst area ~ 1590 cm^2, flow rate 2.0 dm^3 min^{-1}, 400 W mercury lamp.

by a 'cold press' method. We therefore tentatively suggest that the as-purchased Ti substrates have relatively few defects on their surface that can give rise to electron/hole recombination centres in the overlying TiO_2 film, and hence $^{\bullet}OH$-radicals are available for reaction with the model organics. However, once the substrates are polished, the polishing process introduces a high density of surface defects, which results in the efficiency of the organic photooxidation process decreasing dramatically. Thus, in the case of the sol gel film in Fig. 9, the open circuit and +1.0 V runs are almost identical, and show greater degradation than the blank. This suggests that the degradation is purely as a result of photochemical degradation, and that no EFE effect is observed. This is consistent with the EFE effect observed with the unpolished films being due to the underlying thermal TiO_2 film. Such a film is inactive on a polished substrate due to the large number of defect sites introduced by the polishing process. This hypothesis is supported by the results depicted in Fig. 10, which show a degradation of 4-chlorophenol in the larger VR by an unpolished titanium substrate used to fabricate a sol–gel TiO_2 film, but which has had the sol–gel component of the coating removed by thorough rubbing. This time, the blank and open circuit runs exactly overlie, as in Fig. 8, but there is a clear EFE effect, resulting from the thermal film formed on the substrate, and visible as a blue 'sheen', during the annealing process.

The production of intermediates in Figs 9 and 10 was reasonably similar to that shown in Fig. 8(b), an increase in the concentration of the principal intermediate, chlorocatechol or phenol, both of which show the same retention time in the HPLC[33], to ~ 70~90 μM, followed by a decline.

It is clear that the application of the photocatalyst in the form of an immobilized film does entail problems, primarily of the mass transport of species to the catalyst surface, but also with the positioning of the reference electrode, and the position and size of the counter electrode. Any commercial system would almost certainly involve a two-electrode, rather than three-electrode, system, so the problem of the reference electrode is not important. The mass transport problem can be addressed to a certain extent by employing a window that restricts the thickness of the solution layer, and this is currently under investigation. However, it may prove necessary to move to an alternative reactor type, possibly by employing a trickle cell design, particularly if a more highly porous form of TiO_2 is employed. To this end, we recently reported [34] the extremely high photoelectrocatalytic activity of a TiO_2 aerogel towards the mineralization of organics, and have since succeeded in generating the aerogel as a film on a stainless steel substrate. The position and size of the counter electrode is a significant consideration in reactor operation, and may be addressed by moving to other designs, again possibly using a trickle cell design, or by moving towards mesh electrodes, with the counter electrode held behind the working electrode allowing irradiation from the front.

The above problems notwithstanding, real progress has been made. This was highlighted by an experiment carried out using 778 μM 4-chlorophenol in water in the large vortex reactor, and employing two 20W u.v.-B lamps (Phillips) instead of the 400 W

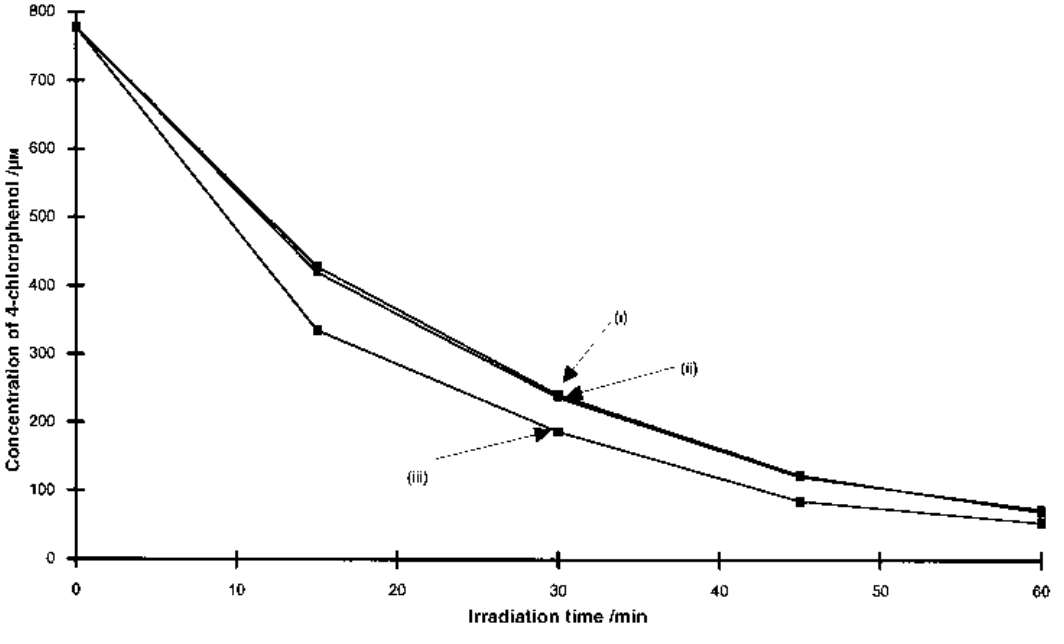

Fig. 10. Concentration of 4-chlorophenol present as a function of irradiation time in the larger vortex reactor (i) in the absence of a photocatalytic film, (ii) in the presence of a sol–gel TiO_2 film on an unpolished Ti substrate, but after the sol–gel film had been rubbed off, at open circuit and (iii) at +1.0 V vs SCE. Reservoir contained 778 μM 4-chlorophenol in 5 dm^3 of water. Catalyst area ~ 1590 cm^2, flow rate 2.0 dm^3min^{-1}, 400 W mercury lamp.

source. After 60 min irradiation of a thermal film and with a +1 V bias, the HPLC showed 23% degradation. Coincidentally, access to TOC analysis had been recently acquired, and the TOC analysis showed a 29% decrease in total organic carbon content.

5. Conclusions

We have succeeded in developing fabrication methods for thermal and sol–gel TiO_2 films on titanium supports up to 45 cm in diameter, and for anodic films up to 30 cm in diameter, and the importance of substrate pretreatment has been highlighted. Our work has shown that the photoelectrochemical reactor design currently employed, the vortex reactor, does not exhibit ideal mass transport characteristics, and possible approaches to solving this problem have been identified. Our results clearly show that electric field enhancement can be observed, in which the degradation of model organic compounds is increased by the application of a potential bias to the *n*-TiO_2 working electrode; however, improvements in the efficiency of the detoxification process are effectively restricted by the poor mass transport characteristics of the current reactor design.

The results obtained in the absence of electrolyte are extremely surprising, suggesting that the efficiency of the photodegradation process is significantly enhanced in the presence of a positive potential bias on the semiconductor, even though no internal electric field is expected to be present in the TiO_2 under these conditions. Furthermore, there is no apparent induction period during which species may have been generated that might enhance the conductivity of the electrolyte. This effect is under ongoing investigation.

Acknowledgements

The authors should like to thank the EPSRC (formally the SERC) and BNFL for funding.

References

[1] 'Framework directive on pollution caused by certain dangerous substances discharged into aquatic environment of the Community'. EEC Directive 76/464/EEC L129, May (1976).
[2] M. A. Callahan, M. Slimak, N. Gbel, I. May, C. Fowler, R. Freed, P. Jennings, R. Dupree, F. Whitmore, B. Maestri, B. Holt and C. Gould, Water Related Environmental Fate of 129 Priority Pollutants.' Report EPA-44014-79-029a, b, NTIS.
[3] F. A. DiGiano, *in* 'Control of Organic Substances in Water and Wastewater' (edited by B. B. Berger, Noyes Data Corporation, New Jersey (1987) ch. 3.
[4] J. J. Rook, *Water Treatment and Examination* **23** (1974) 234.
[5] T. A. Bellar, J. J. Lichtenberg and R. C. Kroner, *J. American Water Works Assoc.* **66** (1974) 703.
[6] J. J. Rook, *Environ. Sci. Tech.* **11** (1977) 478.
[7] Abstracts of the First International Conference on Advanced Oxidation Technologies for Water and Air oxidation, London, Ontario, Canada, 25–30 June (1994).
[8] A. Mills, R. H. Davies and D. Worsley, *Chem. Soc. Rev.* **22** (1993) 417–25.
[9] Y. Zhang, J. C. Crittenden and D. W. Hand, *Chemistry and Industry* **18** (1994) 701–36.
[10] M. A. Fox, S. Ruberu, A. Hadd and Y-S. Kim, *in* Proceedings of the Symposium on Environmental Aspects of Electrochemistry and Photoelectrochemistry (edited by M. Tomkiewicz, R. Haynes, Y. Hori and H. Yoneyama), The Electrochemical Society, **93** (1993) pp. 104–46.
[11] H. Gerischer, *Electrochim. Acta* **38** (1993) 3.
[12] A. Hamnett, *Faraday Disc. Chem. Soc.* **70** (1980) 127; J. Gautron, P. Lemasson and J. F. Marucco, *ibid* (1980) 87.
[13] S. L. Wilkinson and W. A. Anderson, *in* Abstracts of the First International Conference on Advanced Oxidation Technologies for Water and Air Oxidation, London, Ontario, Canada, 25–30 June (1994) p. 299.
[14] K. Hashimoto and A. Fujishima, *in* Abstracts of the First International Conference on Advanced Oxidation Technologies for Water and Air Oxidation, London, Ontario, Canada, 25–30 June (1994) p. 311.
[15] J. F. Kenneke and W. H. Glaze, *in* Proceedings of the Symposium on Water Purification by Photocatalytic, Photoelectrochemical and Electrochemical Process, The Electrochemical Society **94** (1994) p. 365.
[16] A. Hamnett, *Comp. Chem. Kin.* **27** (1987) 61.
[17] K. Vinodgopal, S. Hotchandani and P. V. Kamat, *J. Phys. Chem.* **97** (1993) 9040.
[18] K. Vinodgopal, U. Stafford, K. A. Gray and P. V. Kamat, Proceedings of the Symposium on Water Purification by Photocatalytic, Photoelectrochemical and Electrochemical Processes, The Electrochemical Society **94** (1994) p. 332.
[19] D. H. Kim and M. A. Anderson, *Environ. Sci. Technol.* **28** (1994) 479.
[20] J. S. Anderson and B. G. Hyde, *J. Phys. Chem. Solids* **28** (1967) 1393.
[21] P. Salvador, M. L. García González and F. Muñoz, *J. Phys. Chem.* **96** (1992) 10349.
[22] M. L. García González and P. Salvador, *J Electroanal. Chem.* **325** (1992) 369.
[23] M. Pujades and P. Salvador, *J. Electrochem. Soc.* **136** (1989) 716.
[24] P. A. Christensen, A. Hamnett, K. E. Shaw, G. M. Walker and S. A. Walker, in preparation.
[25] T. Yoko, A. Yuasa, A. Kamiya and S. Sakka, *J. Electrochem. Soc.* **138** (1991) 2279.
[26] C. S. McMillan, J. P. H. Sukamto and W. H. Smyrl, *Faraday Disc. Chem. Soc.* **94** (1992) 63.
[27] J. F. McAleer and L. M. Peter, *Faraday Disc. Chem. Soc.* **70** (1980) 67.
[28] K. Rajeshwar, P. Singh and J. DuBow, *Electrochim. Acta* **23** (1978) 1125.
[29] AEA Technology, 'Powder Fluidic Precipitation', information leaflet.
[30] J. G. Calvert and J. N. Pitts, '*Photochemistry*', Wiley, New York (1960) p. 780.
[31] T. Yoko, A. Yuasa, K. Kamiya and S. Saka, *J. Electrochem. Soc.* **138** (1991) 2279.
[32] J. G. Mavroides, D. I. Tchernev, J. A. Kafalas and D. F. Kolesar, *Mat. Res. Bull.* **10** (1975) 1023.
[33] K. A. Gray, oral presentation, World Environmental Congress, London, Ontario, Canada, 17–22 Sept. (1995). Abstract, p 237.
[34] S. A. Walker, P. A. Christensen, K. E. Shaw and G. M. Walker, *J. Electroanal. Chem.* **393** (1995) 137.